

Bending analysis of different material distributions of functionally graded beam

S. M. Aldousari¹

Received: 10 December 2016 / Accepted: 15 February 2017 / Published online: 1 April 2017
© Springer-Verlag Berlin Heidelberg 2017

Abstract Most analyses of functional graded materials (FGM) focusing on power law distribution, which presents stress concentration at the interface when material properties change rapidly. The objective of the current paper is to develop two symmetric and anti-symmetric functions and compare their effects on the static deflection and bending stresses with classical power-law distribution. The proposed distributions are a symmetric power-law and a sigmoid function which is anti-symmetric. To homogenized micromechanical properties of FGM, the effective material properties are derived on the basis of Voigt model. Kinematic relation of Euler–Bernoulli beam is assumed and virtual work is proposed to derive the equilibrium equations. A finite element model is proposed to form stiffness matrix and force vector and then solve the problem numerically. Proposed model has been validated. Numerical results presents the effect of power exponent, and elasticity ratios on a static deflection and stresses of FG beams. The most significant finding is that, the symmetric power function is more reliable and can considerably reduce the stress than the other two functions. However, the sigmoid function distribution represents the highest stress.

1 Introduction

Functionally graded material (FGM) was first proposed by Japanese scientists to decrease the thermal stresses in

propulsion and airframe structural systems of astronomical flight vehicles [33]. Functionally graded materials (FGMs) are considered a special class of composite materials characterized by smooth and continuous distribution of material properties. They have comparatively smaller residual stresses, lower stress concentrations, and higher bonding strength than conventional composite laminates. Due to these advantages, FGMs are being used increasingly in many applications, such as, in aircraft industry, space vehicles, reactor vessels, automobile, electronics, optics, chemistry, biomedical engineering, nuclear engineering and mechanical engineering [23].

In the microscopic scale, FGM is considered a heterogeneous material, which should be homogenized accurately to be easily modeled computationally. Anthoine [2] presented a second-order homogenization of functionally graded materials. Lee and Kim [35] exploited Voigt rule (VR) and Mori–Tanaka method (MTM) to detect the effective material properties of heterogeneous micromechanical FGM. Effective properties of FG panels are investigated for the two types of models, namely, power function (P-FGM) and sigmoid function (S-FGM) functions.

Chi and Chung [17] suggested a sigmoid function, a combination of two type of P-FGM functions, to reduce the stress intensity factors in a crack structure. In 2003, Chakraborty et al. [16] studied static, free vibration and wave propagation of exponential and power-law FGM Timoshenko beam (TBT) by finite element method (FEM). Li et al. [36] proposed a unified approach to the formulation of TBT and Euler–Bernoulli’s (EB). Kapuria et al. [32] fabricated multi-layered FG beam using powder metallurgy and thermal spraying techniques, and then experimentally validated the results on static and free vibration. Benatta et al. [8] presented an analytical solution for static bending of simply supported FGM hybrid beams using higher-order

✉ S. M. Aldousari
sdossary@kau.edu.sa; saadmaldousari@gmail.com

¹ Department of Mechanical Engineering, Faculty of Engineering, King Abdulaziz University, P.O. Box 80204, Jeddah 21589, Saudi Arabia

shear deformation (HOSD) beam theory. Ben-Oumrane et al. [10] presented a theoretical analysis of flexional bending of Al/Al₂O₃ S-FGM thick beams according to different beam theories. Simsek [52] investigated static analysis of FG simply-supported beam subjected to a uniformly distributed load using Ritz method within the framework of TBT and the HOSD theories. Mahi et al. [42] presented exact solutions to study the free vibration of a unified HOSD beam with temperature-dependent material properties. The materials distributions are varied continuously through the thickness according to an exponential function (E-FGM) or S-FGM. Giunta et al. [25] proposed several axiomatic refined theories for the linear static analysis of beams made of materials whose properties are graded along one or two directions. Huang and Li [30] studied free vibration of non-uniform axially FG beams by transforming the governing differential equation to Fredholm integral equations.

Alshorbagy et al. [1] investigated the free vibration characteristics of P-FGM distributed through beam thickness or beam length using FEM. Birsan et al. [11] employed the direct approach to analyze the deformation of curved FG rods and beams. Shahba and Rajasekaran [51] studied free vibration and stability of axially FG tapered Euler–Bernoulli beams by conventional differential transform method (DTM). Mena et al. [43] derived analytical solutions for static shear correction factor of FG rectangular beams using the energy equivalence principle. Mohanty et al. [45] presented the evaluation of static and dynamic behavior of P-FGM ordinary and sandwich beam using FEM and TBT. Li and Batra [38] derived analytical relations between the critical buckling load of an FGM Timoshenko beam and that of the corresponding homogeneous Euler–Bernoulli beam subjected to axial compressive load for different boundary conditions. Pradhan and Chakraverty [48] investigated free vibration of Euler and Timoshenko P-FGM beams using Rayleigh–Ritz method. Li et al. [39] derived analytically the bending solutions of FGM of TBT in terms of the homogenous Euler–Bernoulli beams. Daouadji et al. [18] derived elasticity solution of a cantilever FG beam with P-FGM and E-FGM subjected to linearly distributed load. Duc and Cong [20] presents a proposal to investigate the nonlinear dynamic response of imperfect symmetric thin S-FGM subjected to mechanical loads. Wang and Wang [57] presented static analysis of higher order sandwich beams by weak form quadrature element method. Liu and Shu [40] investigated analytically free vibrations of E-FGM Euler–Bernoulli beams with a single delamination. Sarkar and Ganguli [50] derived closed-form solutions for axially-loaded FG Timoshenko beams having uniform cross-section and fixed–fixed boundary condition. Jin and Wang [31] studied free vibration of FG Euler–Bernoulli beam using a weak form of DQM. Bourada et al.

[14] presented a new simple shear and normal deformations theory for FG beams. Nguyen et al. [47] studied lateral buckling analysis of thin-walled functionally graded open-section beams. For a nano-scale beam, Eltahir et al. [24] presented a review for bending, buckling, vibrations, and wave propagation of nanoscale FG beams. Hamed et al. [26] investigated free vibration behavior of symmetric and sigmoid functionally graded nanobeams. Ebrahimi and Barati [21] developed a dynamic model of smart shear-deformable heterogeneous piezoelectric nanobeams. Ebrahimi and Salari [22] presented dynamic behavior of piezothermo-electrically excited FG nanobeams. The material distribution is assumed to be sigmoid and power-law graded. Azimi et al. [3] studied thermo-mechanical vibration of rotating axially FG nonlocal Timoshenko beam.

The analysis of FG plate structures are considered by many authors, such as, Meziane et al. [44] presented a simple refined theory for buckling and free vibration of exponentially FG plates. Zidi et al. [58] studied hygro-thermo-mechanical bending of FG plate using higher order shear theory. Bousahla et al. [15] and Bellifa [7] considered the neutral axis effect on the bending and vibration of FG plate with higher order shear theory. Hebali et al. [28] and Mahi et al. [42] developed 3D hyperbolic HOSD for the bending and free vibration of P-FGM plates. Yahia et al. [56] studied wave propagation in porous FG plates using HOSD. Tounsi et al. [54], Boudjerba et al. [12] and Hamidi et al. [27] presented a sinusoidal plate theory including stretching effect for thermomechanical bending of FG sandwich plates. By dividing the transverse displacement into bending, shear, and thickness stretching parts, Belabed et al. [4] and Bennoun et al. [9] developed refined plate theory to study vibrations of sandwich FGM plates. Tounsi et al. [55] and Houari et al. [29] proposed 3-unknown non-polynomial shear deformation theory for static, buckling and vibration analyses FGM sandwich plates. Beldjelili et al. [5] studied hygro-thermo-mechanical bending of S-FGM plates resting on variable elastic foundations. For a nano-plate, Belkourisat et al. [6] and Bounouara et al. [13] developed a nonlocal zeroth-order shear deformation theory for free vibration of FG nanoscale plates resting on elastic foundation.

According to the author's knowledge and survey, the static deflection and stress distribution of symmetric power function and sigmoid function are not yet addressed in literature. Thus, the present paper illustrates the bending behavior of rectangular FG beam subjected to transverse loading with different material distributions. The material consists of ceramics (Al₂O₃) and metal (Al) phases varying through the thickness direction. The Equilibrium equations of FG beam are derived using Euler–Bernoulli beam theory and virtual work principle. The paper is organized as follows: The problem formulation is addressed in Sect. 2. The finite element (FE) model and stiffness matrices are derived

in Sect. 3. Code validation and numerical results are discussed in Sect. 4. Summarized concluding remarks are presented in Sect. 5.

2 Problem formulation

In this section, material distribution through the beam thickness according to Voigt rule is assumed, constitutive equations are illustrated and equilibrium equation of FG Euler-beam is derived.

2.1 Spatial material graduation functions

FGMs are manufactured by mixing different material phases continuously through a specific spatial direction. To estimate the effective properties at micromechanics level, the simplest homogenization techniques are Voigt rule Mori and Tanaka [46] and Mori–Tanaka model, Tomota et al. [53]. Although, Voigt rule does not consider the interaction among adjacent inclusions, Mori–Tanaka method (MTM) considered these interactions of neighboring phases at microscopic level, Lee and Kim [35]. According to Li et al. [37] and Komijani et al. [34], the volume fraction of FG materials can be expressed as

$$V_c = \left(\frac{1}{2} + \frac{z}{h}\right)^k \quad (0 \leq k < \infty) \tag{1a}$$

$$V_c + V_m = 1 \tag{1b}$$

where V is the volume fraction, k is a nonnegative power exponent, and subscripts c and m represent the ceramic and metal, respectively. In the current analysis, three functions are assumed to describe the spatial distribution of materials through the thickness direction. The first and simplest one is the power law function P-FGM, which is described by [1, 16, 18, 23, 31]

$$E(z) = E_m V_m + E_c V_c = E_c + (E_m - E_c) \left(\frac{1}{2} + \frac{z}{h}\right)^k \quad \left(-\frac{h}{2} \leq z \leq \frac{h}{2}\right) \tag{2}$$

The modified symmetric power-law function S-P-FGM has the following form [41]

$$E(z) = E_c + (E_m - E_c) \left(\frac{-2z}{h}\right)^k \quad \left(-\frac{h}{2} \leq z \leq 0\right) \tag{3a}$$

$$E(z) = E_c + (E_m - E_c) \left(\frac{2z}{h}\right)^k \quad \left(0 \leq z \leq \frac{h}{2}\right) \tag{3b}$$

The Sigmoid function S-FGM is assumed to be two power-law functions to ensure smooth distribution of stresses [10, 20, 26, 35, 43]. This function is depicted by

$$E(z) = E_m V_m + E_c V_c = E_m + \frac{1}{2}(E_c - E_m) \left(1 + \frac{2z}{h}\right)^k \quad \left(-\frac{h}{2} \leq z \leq 0\right) \tag{4a}$$

$$E(z) = E_m V_m + E_c V_c = E_c - \frac{1}{2}(E_c - E_m) \left(1 - \frac{2z}{h}\right)^k \quad \left(0 \leq z \leq \frac{h}{2}\right) \tag{4b}$$

The FG beam in the current manuscript is composed of aluminum metal [$E_m = 70$ GPa, and Poisson’s ratio (ν_m) of 0.3] and a ceramic of alumina [$E_c = 380$ GPa, and $\nu_c = 0.3$]. Delale and Erdogan [19] proved that the effect of Poisson’s ratio on the deformation is much less than Young’s modulus. So, the Poisson’s ratio is assumed to be constant in this analysis. The distribution of Young modulus through the beam thickness for the three assumed functions is shown in Fig. 1.

The power function distribution shown in Fig. 1a shows an increase in the power index from 0 (the metal phase) to $k=10$ (ceramics rich phase) as the Young modulus increases. Un-symmetric distribution of the material characteristics through the mid-plane ($z=0$) is the main feature of this function. So, the mid-plane is not coincident with neutral plane, Eltaher et al. [23]. But the other two distributions (S-P-FGM and S-FGM) distribution, as illustrated in Fig. 1b, c, are symmetric and anti-symmetric with respect to mid-plane, respectively, and their mid-planes are coincident with the neutral plane.

2.2 Constitutive equations

Based on the Euler–Bernoulli theory, that plane sections perpendicular to the axis of the beam before deformation remain (a) plane, (b) rigid, and (c) rotate such that they remain perpendicular to the (deformed) axis after deformation. The assumptions amount to neglecting the Poisson effect and transverse strains, Reddy [49]. The displacement field can be assumed as:

$$u(x, z) = u_0(x) - z \frac{dw_0(x)}{dx} \tag{5a}$$

$$w(x, z) = w_0(x) \tag{5b}$$

where u and w are the total displacements along the coordinate (x), and u_0 and w_0 denote the axial and transverse displacements of a point on the neutral axis. According to Euler hypothesis, the only nonzero strain is

$$\epsilon_{xx}(x, z) = \frac{d}{dx} \left[u_0(x) - z \frac{dw_0(x)}{dx} \right] = \frac{du_0(x)}{dx} - z \frac{d^2 w_0(x)}{dx^2} = \epsilon_{xx}^0 + z \epsilon_{xx}^1 \tag{6}$$

And the nonzero stress can be described by

$$\sigma_{xx}(x, z) = E(z) \epsilon_{xx}(x, z) = E(z) [\epsilon_{xx}^0 + z \epsilon_{xx}^1] \tag{7}$$

Axial and bending moment can be written as

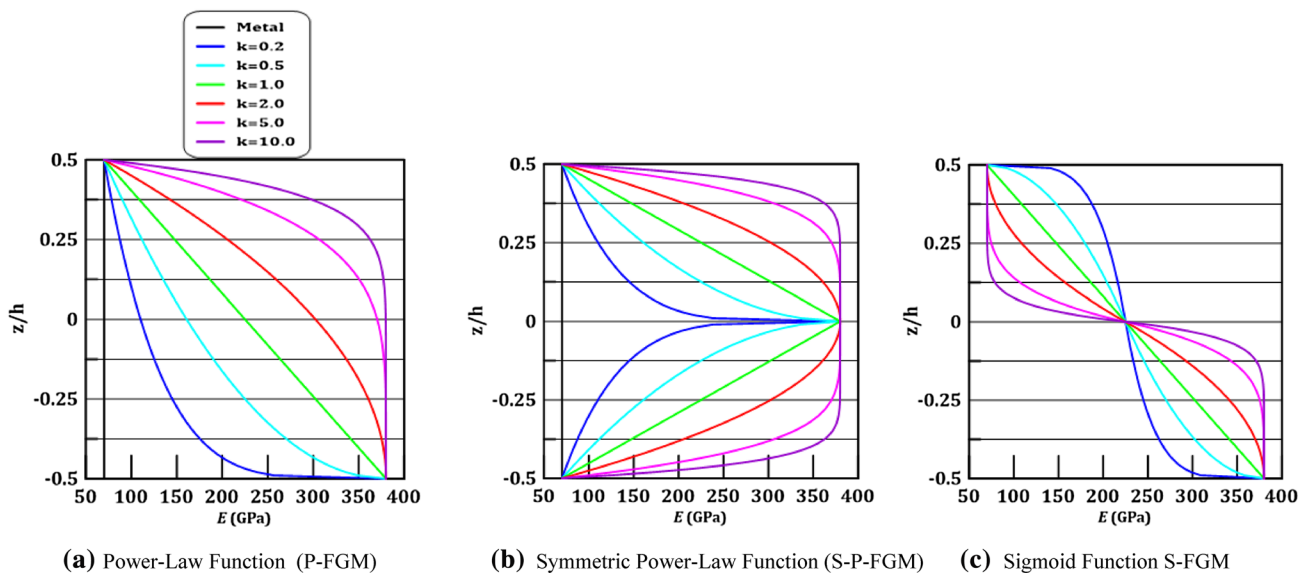


Fig. 1 The variation of Young Modulus through the beam thickness. **a** Power-Law Function (P-FGM). **b** Symmetric Power-Law Function (S-P-FGM). **c** Sigmoid Function S-FGM

$$N_{xx} = \int_A \sigma_{xx} dA = A_{11} \epsilon_{xx}^0 + B_{11} \epsilon_{xx}^1 \tag{8a}$$

$$M_{xx} = \int_A z \sigma_{xx} dA = B_{11} \epsilon_{xx}^0 + D_{11} \epsilon_{xx}^1 \tag{8b}$$

where

$$[A_{11}, B_{11}, D_{11}] = \int_A E(z) [1, z, z^2] dA \tag{9}$$

Based on the principle of virtual work which states that “if a body is in equilibrium, the total virtual work done by internal as well as external forces through their respective virtual displacements is zero”. The analytical form of virtual work is represented by

$$\delta W_T^e = \delta W_I^e - \delta W_E^e = 0 \tag{10}$$

where the internal strain energy is given by

$$\begin{aligned} \delta W_I^e &= \int_V \delta \epsilon_{xx} \sigma_{xx} dV = \int_0^L \int_A (\delta \epsilon_{xx}^0 + z \delta \epsilon_{xx}^1) \sigma_{xx} dA dx \\ &= \int_0^L \int_A \left[\left(\frac{d\delta u_0}{dx} + \frac{dw_0}{dx} \frac{d\delta w_0}{dx} \right) - z \frac{d^2 \delta w_0(x)}{dx^2} \right] \sigma_{xx} dA dx \tag{11} \\ &= \int_0^L \left[\left(\frac{d\delta u_0}{dx} + \frac{dw_0}{dx} \frac{d\delta w_0}{dx} \right) N_{xx} - \frac{d^2 \delta w_0(x)}{dx^2} M_{xx} \right] dx \end{aligned}$$

and work done by external forces is

$$\delta W_E^e = \int_0^L q \delta w_0 dx + \int_0^L f \delta u_0 dx + Q \delta \Delta \tag{12}$$

in which $q(x)$ is the distributed transverse load, $f(x)$ is the distributed axial force, Q is the applied point load, and $\delta \Delta$

is the virtual displacement. By substituting Eqs. (11 and 12) into Eq. (10), and performing integration by parts, yields

$$\begin{aligned} \int_0^L \left\{ \left(\frac{dN_{xx}}{dx} - f \right) \delta u_0 - \left[\frac{d}{dx} \left(\frac{dw_0}{dx} N_{xx} \right) + \frac{d^2 M_{xx}}{dx^2} + q \right] \delta w_0 \right\} dx + \\ \left[N_{xx} \delta u_0 + \left(\frac{dw_0}{dx} N_{xx} + \frac{dM_{xx}}{dx} \right) \delta w_0 - M_{xx} \frac{d\delta w_0}{dx} \right]_0^L - Q \delta \Delta = 0 \tag{13} \end{aligned}$$

Thus, the governing equilibrium equations in terms of forces and moments can be described by

$$\delta u_0: \frac{dN_{xx}}{dx} - f = 0 \tag{14a}$$

$$\delta w_0: \frac{d}{dx} \left(\frac{dw_0}{dx} N_{xx} \right) + \frac{d^2 M_{xx}}{dx^2} + q = 0 \tag{14b}$$

Equilibrium equations in terms of displacements can be described by

$$A_{11} \frac{d^2 u_0}{dx^2} + B_{11} \frac{d^3 w_0}{dx^3} - f = 0 \tag{15a}$$

$$\begin{aligned} A_{11} \left(\frac{du_0}{dx} \frac{d^2 w_0}{dx^2} + \frac{d^2 u_0}{dx^2} \frac{dw_0}{dx} \right) \\ + B_{11} \left(\frac{d^3 u_0}{dx^3} + \frac{d^2 w_0}{dx^2} \frac{d^2 w_0}{dx^2} + \frac{dw_0}{dx} \frac{d^3 w_0}{dx^3} \right) \\ + D_{11} \frac{d^4 w_0}{dx^4} + q = 0 \tag{15b} \end{aligned}$$

3 Numerical FE formulation

The displacement field at the mid-plane of the FG beam can be assumed as

Axial displacement,

$$u_0(x) = \sum_{j=1}^2 u_j \psi_j(x) \tag{16a}$$

Transverse displacement,

$$w_0(x) = \sum_{j=1}^4 w_j \phi_j(x) \tag{16b}$$

where ψ_j is the linear Lagrange interpolation function, and ϕ_j is the Hermite cubic interpolation functions. u_j and w_j are the axial and transverse nodal displacement, respectively. According to Eq. (13), the virtual work statements can be expressed in terms of generalized displacement (u_0, w_0) as

$$\int_0^L \int_A E(z) \left[\left(\frac{d\delta u_0}{dx} + \frac{dw_0}{dx} \frac{d\delta w_0}{dx} \right) - z \frac{d^2 \delta w_0(x)}{dx^2} \right] \left[\frac{du_0(x)}{dx} - z \frac{d^2 w_0(x)}{dx^2} \right] dA dx - \int_0^L q \delta w_0 dx + \int_0^L f \delta u_0 dx + Q \delta \Delta = 0 \tag{17}$$

Substituting Eq. (16) into Eq. (17) results in the following equilibrium equation in matrix form:

$$[K_{uu} + K_{uw} + K_{wu} + K_{ww}] \{d\} = \{f\} + \{q\} + \{Q\} \tag{18}$$

where K_{uu} is the axial stiffness, K_{uw} and K_{wu} is the coupling axial-bending stiffness, K_{ww} is the bending stiffness, $\{f\}$, $\{q\}$ and $\{Q\}$ are the axial, transverse distributed loads and concentrated load vectors, respectively.

4 Numerical results

The results of the proposed model are compared with previous published works to validate the code and model in

the first subsection. After that, the effects of elasticity ratio and power index exponent, on the transverse deflection and axial stresses are investigated for the three proposed function distributions.

4.1 Validation

The geometrical dimensions of the beam in this subsection are proposed by Simsek [52], for a slenderness ratio $L/h=16$. The present results are illustrated in Table 1. As concluded from this table, the present results for P-FGM and those of Simsek [52] are close. A small deviation is observed (5% as a maximum), which is there for two reasons. The first is the difference in proposed theories in analysis (Euler in current analysis, Timoshenko in Simsek [52]). The second reason is due to the dimension of the beam ($L/h=16$), which is a moderately thick beam, and Euler beam is more efficient for thin beams ($L/h > 20$).

Figure 2 illustrates the effect of material distribution parameter (k) on the normal stress distribution through the beam thickness for different function behaviors. The stress results obtained by Simsek [52] is also compared with the proposed power function as shown in Fig. 2a. The obtained results are approximately identical to those obtained by Simesk [52]. The small deviation is again due to the difference in the proposed theories.

4.2 Effect of power index (k)

It is noted from Table 1 that, as power index increases the deflection decreases for both P-FGM and S-P-FGM. Because the ceramics phase which has a higher modulus increases in constituent of the beam, the maximum deflection for S-P-FGM is higher than P-FGM. That means the distribution of ceramics phase in S-P-FGM is less than the distribution in P-FGM at the same power index value. By comparing S-FGM with P-FGM, it is noted that the deflection increases with increasing the power index for S-FGM. However, an opposite effect is observed for P-FGM. As shown in Fig. 2, the higher stress is observed for P-FGM with relative the two other distribution. A symmetric and

Table 1 Maximum non-dimensional transverse deflection of the beam for various power exponent

Power exponent (k)	Maximum non-dimensional transverse deflection			
	Simsek [52]	Present P-FGM	Present S-P-FGM	Present S-FGM
Full metal	1.00812	1.00000	1.00000	1.00000
0.2	0.75595	0.72962	0.896	0.51959
0.5	0.63953	0.60030	0.79032	0.52259
1.0	0.56615	0.52718	0.68293	0.52719
2.0	0.50718	0.47908	0.57377	0.53274
5.0	0.44391	0.43200	0.46281	0.5379
Full Ceramic	0.35284	0.35000	0.35000	0.35000

uniform stress distribution is noted for S-P-FGM, which gives advantage for symmetric power law distribution compared to other functions.

4.3 Effect of elasticity ratio (E1/E2)

Tables 2, 3 and 4 present the maximum deflection of FG beam as the elasticity ratio ranges from 1 to 20 and the material distribution parameter k changes from 0.2 to 10 for the three function distributions: FGM, S-P-FGM and S-FGM, respectively. First of all, when $E1/E2=1$, the isotropic material is rendered. Fixing material distribution parameter k and varying the elasticity ratio results in a significant decrease in deflection for three function distributions. However for the case in hand, the material

distribution parameter has the same effect on P-FGM and S-P-FGM while it has a counter effect on S-FGM at a specific elasticity ratio. For example, at $E1/E2=5$, the static deflection decreases from 0.56098 to 0.23782 (approximately half value) as the power exponent increases from 0.2 to 10 for P-FGM, as seen in Fig. 2. The same observation shows for S-P-FGM, where the deflection decreases from 0.8 to 0.245 (approximately one-third) as the power exponent increases. However, deflection increases from 0.33466 to 0.36513 as the material distribution parameter increases, as shown in Table 4. *The previous observation gives the designer a facility to select the proper distribution and the proper function for his/her application.*

Figure 3 shows the effect of elasticity ratio on the axial stress distribution along the thickness direction for the

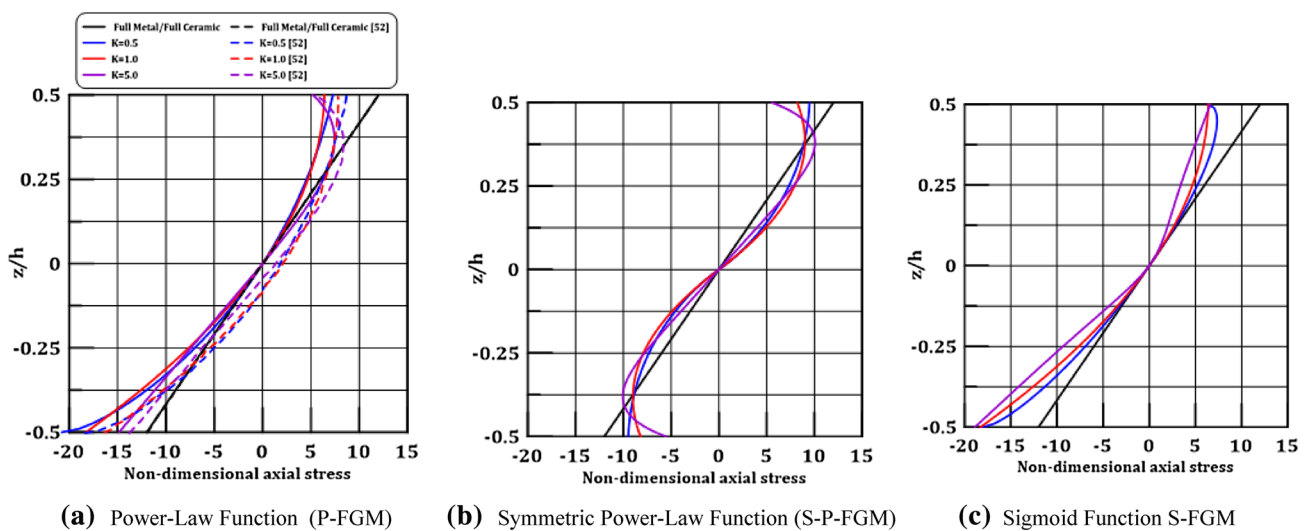


Fig. 2 Maximum Non-dimensional axial stress of the beam for various power exponent. **a** Power-Law Function (P-FGM). **b** Symmetric Power-Law Function (S-P-FGM). **c** Sigmoid Function S-FGM

Table 2 The effect of elasticity ratio and for power exponent on non-dimensional max deflection for P-FGM

$E1/E2$	$k=0.2$	$k=0.5$	$k=0.7$	$k=1.0$	$k=2.0$	$k=5$	$k=10$
1	1.0000	1.0000	1.0000	1.0000	1.0000	1.0000	1.0000
2	0.83224	0.73354	0.70109	0.67179	0.62903	0.58493	0.55482
5	0.56098	0.41616	0.37736	0.34491	0.30115	0.26146	0.23782
10	0.36917	0.24548	0.21596	0.19225	0.16178	0.13617	0.12185
20	0.22261	0.13609	0.11713	0.10237	0.084121	0.069542	0.061688

Table 3 The effect of elasticity ratio and for power exponent on non-dimensional max deflection for S-P-FGM

$E1/E2$	$k=0.2$	$k=0.5$	$k=0.7$	$k=1.0$	$k=2.0$	$k=5$	$k=10$
1	1.0000	1.0000	1.0000	1.0000	1.0000	1.0000	1.0000
2	0.94118	0.875	0.84091	0.8	0.71429	0.61538	0.56522
5	0.8	0.63636	0.56923	0.5	0.38462	0.28571	0.24528
10	0.64	0.4375	0.37	0.30769	0.21739	0.15094	0.12621
20	0.45714	0.26923	0.21765	0.17391	0.11628	0.07767	0.064039

Table 4 The effect of elasticity ratio and for power exponent on non-dimensional max deflection for S-FGM

$E1/E2$	$k=0.2$	$k=0.5$	$k=0.7$	$k=1.0$	$k=2.0$	$k=5$	$k=10$
1	1.0000	1.0000	1.0000	1.0000	1.0000	1.0000	1.0000
2	0.66732	0.66913	0.6703	0.67179	0.67484	0.67755	0.67837
5	0.33466	0.33854	0.34124	0.34491	0.35338	0.36218	0.36513
10	0.18292	0.18628	0.18873	0.19225	0.20125	0.21218	0.21628
20	0.09595	0.098173	0.099859	0.10237	0.10937	0.11914	0.12323

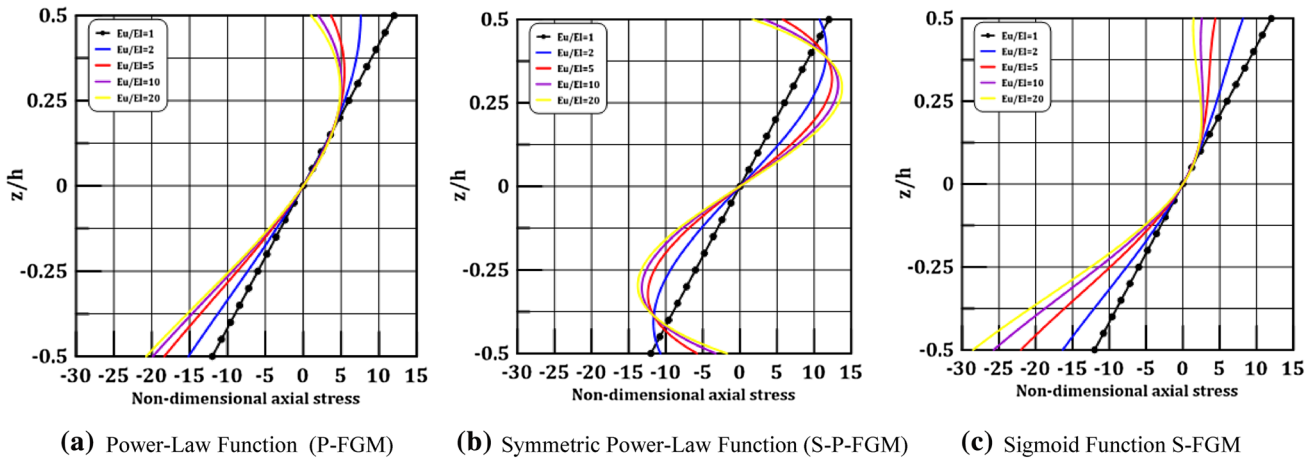


Fig. 3 Non-dimensional axial stress distributions for various elasticity ratios at $k=2.0$. **a** Power-Law Function (P-FGM). **b** Symmetric Power-Law Function (S-P-FGM). **c** Sigmoid Function S-FGM

three proposed functions at a specific power exponent $k=2.0$. As shown in Fig. 3a for P-FGM, as the elasticity ratio increases, the stress increases at the lower surface ($\frac{z}{h} = \frac{-1}{2}$) and decreases at the upper surface ($\frac{z}{h} = \frac{1}{2}$). However, for S-P-FGM, by increasing the elasticity ratio, the stress increases relatively at $\frac{z}{h} = \frac{\pm 1}{4}$ and decreases at upper and lower surfaces, as seen in Fig. 3b. The effect of elasticity ratio on stress distribution for S-FGM is the same as P-FGM. It increases at the lower surface and decreases at the upper one. However, the elasticity ratio is more significant in case of S-FGM than in P-FGM, especially at lower surfaces. Uniform and symmetric distributions are the main features of S-P-FGM.

5 Conclusions

Static bending analysis of an FG simply-supported beam modeled according to Euler–Bernoulli theory and subjected to a uniform distributed load is investigated. Three functions are assumed to describe the variation of metal and ceramics phases through the beam thickness, namely, power function, symmetric power function, and sigmoid function. The equilibrium equations are derived in details according to virtual work and the weak form is proposed

to derive the element stiffness matrices and force vectors using finite element method. The model and results are validated compared to previous work. Numerical results show significant effects of the elasticity ratio and material distribution exponent on the static deflection and stress distribution. Results illustrate a reduction of axial stress for a symmetric power distribution function than for other functions. The proposed model gives designers and engineers a facility to select the proper distributions and proper functions for their application.

Acknowledgements This work was funded by the Deanship of Scientific Research (DSR), King Abdulaziz University, Jeddah, under Grant No. (135-759-D1435). The authors, therefore, acknowledge with thanks DSR technical and financial support.

References

1. A.E. Alshorbagy, M.A. Eltahir, F.F. Mahmoud, Free vibration characteristics of a functionally graded beam by finite element method. *Appl. Math. Modell.* **35**(1), 412–425 (2011)
2. A. Anthoine, Second-order homogenisation of functionally graded materials. *Int. J. Solids Struct.* **47**(11), 1477–1489 (2010)
3. M. Azimi, S.S. Mirjavadi, N. Shafiei, A.M.S. Hamouda, Thermo-mechanical vibration of rotating axially functionally

- graded nonlocal Timoshenko beam. *Appl. Phys. A* **123**(1), 104 (2017)
4. Z. Belabed, M. S. A. Houari, A. Tounsi, S. R. Mahmoud, O. A. Bég, An efficient and simple higher order shear and normal deformation theory for functionally graded material (FGM) plates. *Comp. Part B* **60**, 274–283 (2014)
 5. Y. Beldjelili, A. Tounsi, S.R. Mahmoud, Hygro-thermo-mechanical bending of S-FGM plates resting on variable elastic foundations using a four-variable trigonometric plate theory. *Smart Struct. Systems* **18**(4), 755–786 (2016)
 6. I. Belkorissat, M.S.A. Houari, A. Tounsi, E.A. Bedia, S.R. Mahmoud, On vibration properties of functionally graded nanoplate using a new nonlocal refined four variable model. *Steel Comp. Struct.* **18**(4), 1063–1081 (2015)
 7. H. Bellifa, K.H. Benrahou, L. Hadji, M.S.A. Houari, A. Tounsi, Bending and free vibration analysis of functionally graded plates using a simple shear deformation theory and the concept the neutral surface position. *J. Brazilian Soc. Mech. Sci. Eng.* **38**(1), 265–275 (2016)
 8. M.A. Benatta, A. Tounsi, I. Mechab, M.B. Bouiadjra, Mathematical solution for bending of short hybrid composite beams with variable fibers spacing. *Appl. Math. Comput.* **212**(2), 337–348 (2009)
 9. M. Bennoun, M.S.A. Houari, A. Tounsi, A novel five variable refined plate theory for vibration analysis of functionally graded sandwich plates. *Mech Adv. Mater. Struct.* **23**(4), 423–431 (2016)
 10. S. Ben-Oumrane, T. Abedlouahed, M. Ismail, B.B. Mohamed, M. Mustapha, A.B. El Abbas, A theoretical analysis of flexional bending of Al/Al₂O₃S-FGM thick beams. *Comput. Mater. Sci.* **44**, 1344–1350 (2009)
 11. M. Birsan, H. Altenbach, T. Sadowski, V. A. Eremeyev, D. Pietras, Deformation analysis of functionally graded beams by the direct approach. *Comp. Part B* **43**(3), 1315–1328 (2012)
 12. B. Boudierba, M.S.A. Houari, A. Tounsi, Thermomechanical bending response of FGM thick plates resting on Winkler-Pasternak elastic foundations. *Steel Comp. Struct.* **14**(1), 85–104 (2013)
 13. F. Bounouara, K.H. Benrahou, I. Belkorissat, A. Tounsi, A nonlocal zeroth-order shear deformation theory for free vibration of functionally graded nanoscale plates resting on elastic foundation. *Steel Comp. Struct.* **20**(2), 227–249 (2016)
 14. M. Bourada, A. Kaci, M.S.A. Houari, A. Tounsi, A new simple shear and normal deformations theory for functionally graded beams. *Steel Comp. Struct.* **18**(2), 409–423 (2015)
 15. A.A. Bousahla, M.S.A. Houari, A. Tounsi, E.A. Adda-Bedia, A novel higher order shear and normal deformation theory based on neutral surface position for bending analysis of advanced composite plates. *Int. J. Comput. Methods* **11**(06), 1350082 (2014)
 16. A. Chakraborty, S. Gopalakrishnan, J.N. Reddy, A new beam finite element for the analysis of functionally graded materials. *Int. J. Mech. Sci.* **45**(3), 519–539 (2003)
 17. S.H. Chi, Y.L. Chung, Cracking in sigmoid functionally graded coating. *J Mech* **18**, 41–53 (2002)
 18. T.H. Daouadji, A.H. Henni, A. Tounsi, A.B. El Abbes, Elasticity solution of a cantilever functionally graded beam. *Appl. Compos. Mater.* **20**(1), 1–15 (2013)
 19. F. Delale, F. Erdogan, The crack problem for a nonhomogeneous plane. *J. Appl. Mech.* **50**(3), 609–614 (1983)
 20. N. D. Duc, P. H. Cong, Nonlinear dynamic response of imperfect symmetric thin sigmoid-functionally graded material plate with metal-ceramic-metal layers on elastic foundation. *J. Vib. Control*, **21**(4), 637–646 (2013)
 21. F. Ebrahimi, M.R. Barati, Dynamic modeling of smart shear-deformable heterogeneous piezoelectric nanobeams resting on Winkler–Pasternak foundation. *Appl. Phys. A* **122**(11), 952 (2016)
 22. F. Ebrahimi, E. Salari, Analytical modeling of dynamic behavior of piezo-thermo-electrically affected sigmoid and power-law graded nanoscale beams. *Appl. Phys. A* **122**(9), 793 (2016)
 23. M.A. Eltaher, A.E. Alshorbagy, F.F. Mahmoud, Determination of neutral axis position and its effect on natural frequencies of functionally graded macro/nanobeams. *Compos. Struct.* **99**, 193–201 (2013)
 24. M.A. Eltaher, M.E. Khater, S.A. Emam, A review on nonlocal elastic models for bending, buckling, vibrations, and wave propagation of nanoscale beams. *Appl. Math. Modell.* **40**(5), 4109–4128 (2016)
 25. G. Giunta, S. Belouettar, E. Carrera, Analysis of FGM beams by means of classical and advanced theories. *Mech. Adv. Mater. Struct.* **17**(8), 622–635 (2010)
 26. M.A. Hamed, M.A. Eltaher, A.M. Sadoun, K.H. Almitani, Free vibration of symmetric and sigmoid functionally graded nanobeams. *Appl. Phys. A* **122**(9), 829 (2016)
 27. A. Hamidi, M.S.A. Houari, S.R. Mahmoud, A. Tounsi, A sinusoidal plate theory with 5-unknowns and stretching effect for thermomechanical bending of functionally graded sandwich plates. *Steel Compos. Struct.* **18**(1), 235–253 (2015)
 28. H. Hebbali, A. Tounsi, M.S.A. Houari, A. Bessaim, E.A.A. Bedia, New quasi-3D hyperbolic shear deformation theory for the static and free vibration analysis of functionally graded plates. *J. Eng. Mech.* **140**(2), 374–383 (2014)
 29. M.S.A. Houari, A. Tounsi, A. Bessaim, S.R. Mahmoud, A new simple three-unknown sinusoidal shear deformation theory for functionally graded plates. *Steel Compos. Struct.* **22**(2), 257–276 (2016)
 30. Y. Huang, X.F. Li, A new approach for free vibration of axially functionally graded beams with non-uniform cross-section. *J. Sound Vib.* **329**(11), 2291–2303 (2010)
 31. C. Jin, X. Wang, Accurate free vibration analysis of Euler functionally graded beams by the weak form quadrature element method. *Compos. Struct.* **125**, 41–50 (2015)
 32. S. Kapuria, M. Bhattacharyya, A.N. Kumar, Bending and free vibration response of layered functionally graded beams: a theoretical model and its experimental validation. *Compos. Struct.* **82**(3), 390–402 (2008)
 33. M. F. G. M. Koizumi, FGM activities in Japan. *Compos. Part B* **28**(1), 1–4 (1997)
 34. M. Komijani, S.E. Esfahani, J.N. Reddy, Y.P. Liu, M.R. Eslami, Nonlinear thermal stability and vibration of pre/post-buckled temperature-and microstructure-dependent functionally graded beams resting on elastic foundation. *Compos. Struct.* **112**, 292–307 (2014)
 35. C.Y. Lee, J.H. Kim, Evaluation of homogenized effective properties for FGM panels in aero-thermal environments. *Compos. Struct.* **120**, 442–450 (2015)
 36. X.F. Li, A unified approach for analyzing static and dynamic behaviors of functionally graded Timoshenko and Euler–Bernoulli beams. *J. Sound Vib.* **318**(4), 1210–1229 (2008)
 37. S.R. Li, H.D. Su, C.J. Cheng, Free vibration of functionally graded material beams with surface-bonded piezoelectric layers in thermal environment. *Appl. Math. Mech.* **30**, 969–982 (2009)
 38. S.R. Li, R.C. Batra, Relations between buckling loads of functionally graded Timoshenko and homogeneous Euler–Bernoulli beams. *Compos. Struct.* **95**, 5–9 (2013)
 39. S.R. Li, D.F. Cao, Z.Q. Wan, Bending solutions of FGM Timoshenko beams from those of the homogenous Euler–Bernoulli beams. *Appl. Math. Modell.* **37**(10), 7077–7085 (2013)
 40. Y. Liu, D. W. Shu, Free vibration analysis of exponential functionally graded beams with a single delamination. *Compos. Part B* **59**, 166–172 (2014)

41. A. Mahi, E.A. Bedia, A. Tounsi, I. Mechab, An analytical method for temperature-dependent free vibration analysis of functionally graded beams with general boundary conditions. *Compos. Struct.* **92**(8), 1877–1887 (2010)
42. A. Mahi, E.A. Adda Bedia, A. Tounsi, A new hyperbolic shear deformation theory for bending and free vibration analysis of isotropic, functionally graded, sandwich and laminated composite plates. *Appl. Math. Modell.* **39**, 2489–2508 (2015)
43. R. Mena, A. Tounsi, F. Mouaici, I. Mechab, M. Zidi, E.A.A. Bedia, Analytical solutions for static shear correction factor of functionally graded rectangular beams. *Mech. Adv. Mater. Struct.* **19**(8), 641–652 (2012)
44. M.A.A. Meziane, H.H. Abdelaziz, A. Tounsi, An efficient and simple refined theory for buckling and free vibration of exponentially graded sandwich plates under various boundary conditions. *J. Sandw. Struct. Mater* **16**(3), 293–318 (2014)
45. S.C. Mohanty, R.R. Dash, T. Rout, (2012). Static and dynamic stability analysis of a functionally graded Timoshenko beam. *Int. J. Struct. Stab. Dyn.* **12**(04), 1250025
46. T. Mori, K. Tanaka, Average stress in matrix and average elastic energy of materials with misfitting inclusions. *Acta metallurgica* **21**(5), 571–574 (1973)
47. T.T. Nguyen, P.T. Thang, J. Lee, Lateral buckling analysis of thin-walled functionally graded open-section beams. *Compos. Struct.* **160**, 952–963 (2017)
48. K. K. Pradhan, S. Chakraverty, Free vibration of Euler and Timoshenko functionally graded beams by Rayleigh–Ritz method. *Compos. Part B* **51**, 175–184 (2013)
49. J.N. Reddy, *An Introduction to Nonlinear Finite Element Analysis: With Applications to Heat Transfer, Fluid Mechanics, and Solid Mechanics.* (Oxford university press, Oxford, 2014)
50. K. Sarkar, R. Ganguli, Closed-form solutions for axially functionally graded Timoshenko beams having uniform cross-section and fixed–fixed boundary condition. *Compos. Part B* **58**, 361–370 (2014)
51. A. Shahba, S. Rajasekaran, Free vibration and stability of tapered Euler–Bernoulli beams made of axially functionally graded materials. *Appl. Math. Modell.* **36**(7), 3094–3111 (2012)
52. M. Şimşek, Static analysis of a functionally graded beam under a uniformly distributed load by Ritz method. *Int J Eng Appl Sci* **1**(3), 1–11 (2009)
53. Y. Tomota, K. Kuroki, T. Mori, I. Tamura, Tensile deformation of two-ductile-phase alloys: Flow curves of α - γ Fe-Cr-Ni alloys. *Mater. Sci. Eng.* **24**(1), 85–94 (1976)
54. A. Tounsi, M.S.A. Houari, S. Benyoucef, A refined trigonometric shear deformation theory for thermoelastic bending of functionally graded sandwich plates. *Aerosp. Sci. Technol.* **24**(1), 209–220 (2013)
55. A. Tounsi, M.S.A. Houari, A. Bessaim, A new 3-unknowns non-polynomial plate theory for buckling and vibration of functionally graded sandwich plate. *Struct. Eng. Mech. Int. J.* **60**(4), 547–565 (2016)
56. S. A. Yahia, H. A. Atmane, M. S. A. Houari, A. Tounsi, Wave propagation in functionally graded plates with porosities using various higher-order shear deformation plate theories. *Struct. Eng. Mech.* **53**(6), 1143–1165 (2015)
57. Y. Wang, X. Wang, Static analysis of higher order sandwich beams by weak form quadrature element method. *Compos. Struct.* **116**, 841–848 (2014)
58. M. Zidi, A. Tounsi, M. S. A. Houari, O. A. Bég, Bending analysis of FGM plates under hygro-thermo-mechanical loading using a four variable refined plate theory. *Aerosp. Sci. Technol.* **34**, 24–34 (2014)